

The 2-Norbornyl Cation via the Fragmentations of *exo*- and *endo*-2-Norbornyloxchlorocarbenes: Distinction without Much Difference

Robert A. Moss,^{*,‡} Fengmei Zheng,[‡] Ronald R. Sauers,^{*,‡} and John P. Toscano[§]

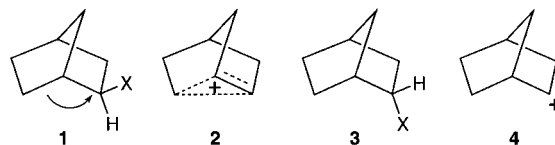
Contribution from the Departments of Chemistry, Rutgers, The State University of New Jersey, New Brunswick, New Jersey 08903, and Johns Hopkins University, Baltimore, Maryland 21218

Received March 5, 2001. Revised Manuscript Received May 15, 2001

Abstract: *exo*- and *endo*-2-norbornyloxchlorocarbenes (**7**) were generated photochemically from the corresponding diazirines (**6**). Both carbenes fragmented to [2-norbornyl cation (carbon monoxide) chloride] ion pairs in MeCN or 1,2-dichloroethane solutions. Products included *exo*-norbornyl chloride (**8**), *endo*-norbornyl chloride (**9**), norbornene (**10**), and nortricyclene (**11**). Fragmentation activation energies were very low (<~4 kcal/mol) and, as a result, the (laser flash photolytic) rate constants for fragmentation were essentially identical for *exo*-**7** and *endo*-**7** (~5 × 10⁵ s⁻¹ in MeCN). Due to chloride return within the ion pairs, product distributions from *exo*- and *endo*-**7** differed, with more *endo*-chloride formed from the *endo*-carbene: the **8/9** product ratio in MeCN was ~41 from *exo*-**7**, but only 4.6 from *endo*-**7**. Norbornene, formed by proton transfer to Cl⁻ within the ion pairs, was a major product in both cases (44% from *exo*-**7** and 62% from *endo*-**7**). In MeOH/MeCN, up to 28% of *exo*-2-norbornyl methyl ether formed at the expense of some of the norbornene, but even in 100% MeOH, the norbornyl chloride products of ion pair return still accounted for 46% and 31% of the *exo*-**7** and *endo*-**7** product mixtures (accompanied by 26–32% of norbornene). Electronic structure calculations on the ground states and fragmentation transition states of *exo*-**7** and *endo*-**7** are presented.

The structure of the 2-norbornyl cation (and of the transition states leading to it in solvolytic reactions) evoked heated arguments among organic chemists of the highest repute.¹ Indeed, the “nonclassical ion” debate “ranks among the classics of chemical disagreements. It was fought out nationally and internationally...through seminars, meetings, referees reports, papers, books, and private communications.”^{2,3}

It now seems clear that *exo*-2-norbornyl derivatives (**1**) do solvolyze with significant participation of the C1–C6 σ electrons to yield a “nonclassical” 2-norbornyl cation (**2**), in which C1, C2, and C6 comprise a 3-center, 2-electron bonding array.^{3,4} In solvolysis reactions, C1–C6 σ participation favors *exo* substrates **1** by 4–7 kcal/mol^{4c} over *endo* substrates (**3**), where such participation is stereoelectronically unfavorable.



Historically, **3** was envisioned to solvolyze via the “classical” 2-norbornyl cation (**4**),³ although **4** is no longer believed to be a minimum on the 2-norbornyl cation energy surface.^{4c,d} However, within the active sites of antibodies elicited from analogues of *endo*-2-norbornyl solvolysis transition states,⁵ or perhaps within tight ion pairs, classical or near-classical 2-norbornyl cations might fleetingly exist, i.e., when external influences supplant and/or mitigate demand on the C1–C6 electron pair for the stabilization of δ^+ at C2.

Typical solvolyses, with $E_a > 20$ kcal/mol, incur significant δ^+ at the norbornyl C2, leading to *exo/endo* rate and activation energy differences. With X = OBs, for example, **1** solvolyzes 350 times faster than **3** in KOAc-buffered acetic acid, a rate advantage that increases to 1610 when corrected for internal return from **1**.^{3c,6} With X = OTs, $\Delta G^\ddagger = 22.6$ kcal/mol for the acetolysis of **1**, but 27.1 kcal/mol for the acetolysis of **3**. Corrected for ground-state energy differences, this corresponds to a free energy difference of 5.8 kcal/mol between the *exo* and *endo* transition states.⁷ With more effective ionizing solvents, the intrinsic *exo/endo* reactivity difference is magnified

[‡] Rutgers University.

[§] Johns Hopkins University.

(1) Brock, W. H. *The Norton History of Chemistry*; Norton: New York, 1992; pp 558–569.

(2) Roberts, J. D. *The Right Place at the Right Time*; American Chemical Society: Washington, DC, 1990; p 89. Cf., ref 1, p 568.

(3) Some synoptic references: (a) Bartlett, P. D. *Nonclassical Ions*; Benjamin: New York, 1965. (b) Brown, H. C. *The Non-Classical Ion Problem* (with comments by Schleyer, P. v. R.); Plenum: New York, 1977. (c) Lowry, T. H.; Richardson, K. S. *Mechanism and Theory in Organic Chemistry*; Harper and Row: New York, 1987; pp 463–478. (d) Arnett, E. M.; Hofelich, T. C.; Shriver, G. W. In *Reactive Intermediates*; Jones, M., Jr.; Moss, R. A., Eds.; Wiley-Interscience: New York, 1985; Vol. 3, pp 189f, especially pp 193–202. (e) Grob, C. A. *Acc. Chem. Res.* **1983**, *16*, 426. (f) Brown, H. C. *Acc. Chem. Res.* **1983**, *16*, 432. (g) Olah, G. A.; Prakash, G. K. S.; Saunders, M. *Acc. Chem. Res.* **1983**, *16*, 440. (h) Walling, C. *Acc. Chem. Res.* **1983**, *16*, 448. (i) Olah, G. A. *Angew. Chem., Int. Ed. Engl.* **1995**, *34*, 1393.

(4) (a) Schleyer, P. v. R.; Sieber, S. *Angew. Chem., Int. Ed. Engl.* **1993**, *32*, 1606. (b) Koch, W.; Liu, B.; DeFrees, D. J. *J. Am. Chem. Soc.* **1989**, *111*, 1527. (c) Schreiner, P. R.; Severance, D. L.; Jorgensen, W. L.; Schleyer, P. v. R.; Schaefer, H. F., III *J. Am. Chem. Soc.* **1995**, *117*, 2663. (d) Perera, S. A.; Bartlett, R. J. *J. Am. Chem. Soc.* **1996**, *118*, 7849.

(5) Ma, L.; Sweet, E. H.; Schultz, P. G. *J. Am. Chem. Soc.* **1999**, *121*, 10227.

(6) (a) Winstein, S.; Trifan, D. S. *J. Am. Chem. Soc.* **1949**, *71*, 2953. (b) Winstein, S.; Trifan, D. S. *J. Am. Chem. Soc.* **1952**, *74*, 1147, 1154. (c) Winstein, S.; Clippinger, E.; Howe, R.; Vogelfanger, E. *J. Am. Chem. Soc.* **1965**, *87*, 376.

(7) Brown, H. C. *Tetrahedron* **1976**, *32*, 179. Cf., ref 3c, p 468.

as demand for C1–C6 σ electron donation increases. Thus, in hexafluoro-2-propanol, **1** ($X = \text{OTs}$) solvolyzes >15 000 times more rapidly than **3**.⁸

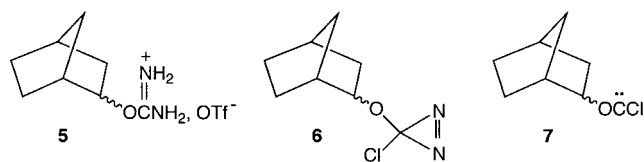
What would happen to the *exo*/*endo* rate difference if electron demand were greatly decreased during heterolysis of the C2–X bond? If leaving group X were made so reactive that the activation energy for C–X heterolysis approached zero, then the kinetic disparity between *exo* and *endo* substrates should disappear. Moreover, product distributions from **1** or **3** might then depend on initial substrate identity, i.e., geometric differences in initially formed ion pairs might be translated into product “memory effects”.

The 2-norbornyl diazonium ions **1** and **3** ($X = \text{N}_2^+$) are appropriate substrates to test the latter idea, and indeed, product variance is observed in the deaminations of **1-NH**₂ and **3-NH**₂.⁹ For example, deamination of optically active **1** ($X = \text{NH}_2$) in water gives racemic **1-OH**, accompanied by less than 0.1% of **3-OH**, whereas **3-NH**₂ gave 10.2% of **3-OH** with complete retention of configuration and 89.8% of nearly racemic **1-OH**.¹⁰ However, the intermediate diazonium ions are so unstable that the kinetics of their nitrogen loss could not be ascertained.

We found that the fragmentation of alkoxyhalocarbenes (ROCX) affords alkyl halides via ion pairs ($\text{R}^+ \text{OCX}^-$), that the product distributions of these processes resemble those of the analogous deaminative reactions ($\text{R}^+ \text{N}_2 \text{X}^-$), and that the kinetics of carbene fragmentation can be determined by laser flash photolysis (LFP).^{11,12} Given the low activation energies associated with fragmentations of ROCCl in solution,^{11,12b,c,13} the fragmentations of the 2-norbornyloxylchlorocarbenes **1** and **3** ($X = \text{OCCl}$) should provide a good look at the consequences of lowering the demand for σ electron stabilization during generation of the 2-norbornyl cation. Descriptions of pertinent experiments follow.

Results

Synthesis and Products. *exo*- and *endo*-2-norborneol were converted to the corresponding *O*-norbornyl isouronium triflates (**5**) by reaction with cyanamide and trifluoromethanesulfonic acid in dry THF (55 °C, 30 h).¹⁴ The isouronium salts were individually oxidized to *exo*- or *endo*-3-chloro-3-(2-norbornyl-



oxy)diazirines, **6**, with 12% aqueous NaOCl solution, saturated with NaCl (~50%, 15 °C, 15 min).¹⁵ Pentane solutions of **6** were dried and purified by chromatography over silica gel with a pentane eluent. They were characterized by UV [*exo*-**6**, λ_{max} 359 nm; *endo*-**6**, λ_{max} 352 nm] and NMR spectroscopy. By

(8) Bentley, T. W.; Bowen, C. T.; Morten, D. H.; Schleyer, P. v. R. *J. Am. Chem. Soc.* **1981**, *103*, 5466. Cf., ref 3c, p 469.

(9) For a review: Zollinger, H. *Diazo Chemistry II*; VCH: Weinheim, Germany, 1995; pp 280–287.

(10) Kirmse, W.; Siegfried, R. *J. Am. Chem. Soc.* **1983**, *105*, 950 and earlier references cited there. See also, ref 9, pp 284–5.

(11) Moss, R. A. *Acc. Chem. Res.* **1999**, *32*, 969.

(12) (a) Moss, R. A.; Ge, C.-S.; Maksimovik, L. *J. Am. Chem. Soc.* **1996**, *118*, 9792. (b) Moss, R. A.; Johnson, L. A.; Merrer, D. C.; Lee, G. E., Jr. *J. Am. Chem. Soc.* **1999**, *121*, 5940. (c) Moss, R. A.; Johnson, L. A.; Yan, S.; Toscano, J. P.; Showalter, B. M. *J. Am. Chem. Soc.* **2000**, *122*, 11256.

(13) Yan, S.; Sauer, R. R.; Moss, R. A. *Org. Lett.* **1999**, *1*, 1603.

(14) Moss, R. A.; Kaczmarczyk, G. M.; Johnson, L. A. *Synth. Commun.* **2000**, *30*, 3233.

(15) Graham, W. H. *J. Am. Chem. Soc.* **1965**, *87*, 4396.

Table 1. Fragmentation Products of *exo*-2-Norbornyloxylchlorocarbene (*exo*-**7**)^a

solvent	additives	8	9	10	11
MeCN	none	49.7	1.2	44.0	5.1
MeCN	0.5 M TBACl ^b	45.8	1.4	47.5	5.3
MeCN	5.77 M pyr ^c	47.3	2.0	45.1	5.5
MeCN	0.5 M TBABF ₄ ^d	49.2	1.2	47.3	2.2
MeCN	0.5 M TBACl + 5.77 M pyr	47.2	1.8	47.9	3.1
DCE ^e	none	50.5	2.0	40.0	7.5
DCE	0.5 M TBACl	43.3	2.4	46.7	7.5
DCE	5.77 M pyr	47.3	1.7	46.3	4.6
DCE	0.5 M TBACl + 5.77 M pyr	46.9	2.6	48.5	2.0

^a All experiments at 25 °C. Product distributions are percentages of the total product mixture. ^b TBACl = tetrabutylammonium chloride. ^c pyr = pyridine. ^d TBABF₄ = tetra-*n*-butylammonium tetrafluoroborate. ^e DCE = 1,2-dichloroethane.

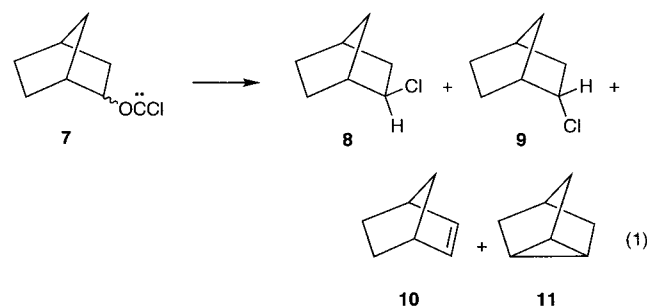
Table 2. Fragmentation Products of *endo*-2-Norbornyloxylchlorocarbene (*endo*-**7**)^a

solvent	additives	8	9	10	11
MeCN	none	28.1	6.1	62.4	3.4
MeCN	0.5 M TBACl	30.0	5.0	61.9	3.1
MeCN	0.5 M TBABF ₄	27.5	6.4	62.6	3.4
MeCN	0.5 M TBACl + 5.77 M pyr	29.0	5.8	60.8	4.4
DCE	none	31.5	6.9	57.0	4.6
DCE	0.5 M TBACl	38.7	4.6	52.1	4.6
DCE	5.77 M pyr	29.4	6.8	61.7	2.0
DCE	0.5 M TBACl + 5.77 M pyr	36.1	5.7	53.4	4.8

^a Conditions and definitions as described in the notes to Table 1.

rotoevaporation of the pentane and replacement with a second solvent, solutions of the diazirines were prepared in MeCN or 1,2-dichloroethane (DCE), where λ_{max} of **6** was 356 nm.

Photolyses ($\lambda_{\text{max}} > 320$ nm) of *exo*- or *endo*-**6** in MeCN or DCE ($A_{356} = 1.0$) at 25 °C generated *exo*- or *endo*-2-norbornyloxylchlorocarbenes, **7**, which fragmented to mixtures of *exo*-2-chloronorbornane (**8**), *endo*-2-chloronorbornane (**9**), norbornene (**10**), and nortricyclene (**11**); cf., eq 1. Products were



identified by GC-MS and by capillary GC spiking experiments with authentic materials; product distributions were obtained by capillary GC analysis; cf., Tables 1 and 2.

Principal observations to be made about the products include the following:

(a) The carbene fragmentations produce very large quantities of norbornene, 40–48% from *exo*-**7** and 52–62% from *endo*-**7**. This is unanticipated; aqueous nitrous acid deamination of *exo*- or *endo*-2-aminonorbornane produces only “minor” quantities of hydrocarbons.¹⁶ The *exo* amine, for example, affords only 1.5% of **10** and/or **11**.^{17,18} Solvolyses of **1** or **3** ($X = \text{OTs}$ or OBs) also afford substitution rather than elimination products.^{6,19}

(16) Berson, J. A.; Remanick, A. *J. Am. Chem. Soc.* **1964**, *86*, 1749.

(17) Corey, E. J.; Casanova, J., Jr.; Vatakencherry, P. A.; Winter, R. J. *Am. Chem. Soc.* **1963**, *85*, 169.

(18) Reference 10 does not mention the formation of **10** or **11**.

Table 3. Fragmentation Products of *exo-7* and *endo-7* in MeCN and MeOH^a

carbene	solvent	8	9	10	11	12
<i>exo-7</i>	MeCN	49.7	1.2	44.0	5.1	0.0
<i>exo-7</i>	MeOH	44.3	1.3	26.1	6.0	22.3
<i>endo-7</i>	MeCN	28.1	6.1	62.4	3.4	0.0
<i>endo-7</i>	MeOH	24.5	6.2	31.5	8.9	28.3

^a At 25 °C. Product distributions are percentages of the total product mixture.

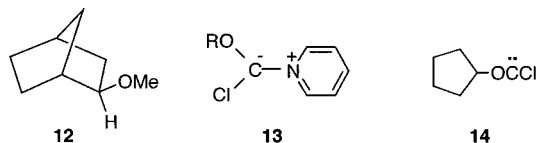
(b) There are clear differences between the product distributions from *exo-7* and *endo-7*. Fragmentation of the *exo* carbene affords more *exo*-chloride **8**, less norbornene, and very little *endo*-chloride **9**. *endo*-Carbene **7** gives norbornene as the major product, 5–6% of the *endo* chloride, and only ~30% of *exo*-chloride **8**. (Significant quantities of nortricyclene are produced from both carbenes.) Indeed, in MeCN, the *exo/endo* (**8/9**) ratio drops from ~41 for the fragmentation of *exo-7* to ~4.6 for *endo-7*.

(c) There is little overt effect of the solvent change from MeCN ($\epsilon = 35.6$) to DCE ($\epsilon = 10.7$), the two solvents employed in the kinetic studies described below.

(d) There are only small changes in the product distributions (relative yields), in either solvent, as a result of adding 0.5 M tetrabutylammonium chloride (TBACl), 0.5 M TBACl + 5.77 M pyridine, 0.5 M tetrabutylammonium fluoborate (TBABF₄), or 5.77 M pyridine. Failure of the added TBACl to markedly increase the share of *endo*-chloride (**9**) from *exo*-carbene **7** suggests that Cl⁻ induced S_N2 fragmentations of **7** are unimportant for the 2-norbornyloxylchlorocarbenes.²⁰

(e) No trapping products^{12a} of carbenes **7** are observed; e.g., neither ROCHCl₂ (HCl trapping), RO(C=O)H (water trapping), nor RNHCOMe (Ritter product from MeCN trapping) are formed. The fragmentations of *exo-7* and *endo-7* are faster than the potential trapping reactions, and the ion pairs (see Discussion) formed from **7** efficiently collapse to **8** and **9**, or “eliminate” HCl to yield **10** or **11**. At high concentrations of pyridine, however, carbenes **7** can be diverted in part to pyridinium ylides; see below.

The Addition of MeOH. When *exo-7* or *endo-7* is generated by the photolysis of *exo-* or *endo-6* in MeOH/MeCN, products **8–11** are accompanied by *exo-2*-norbornyl methyl ether (**12**), identified by GC and GC-MS comparisons with an authentic sample.

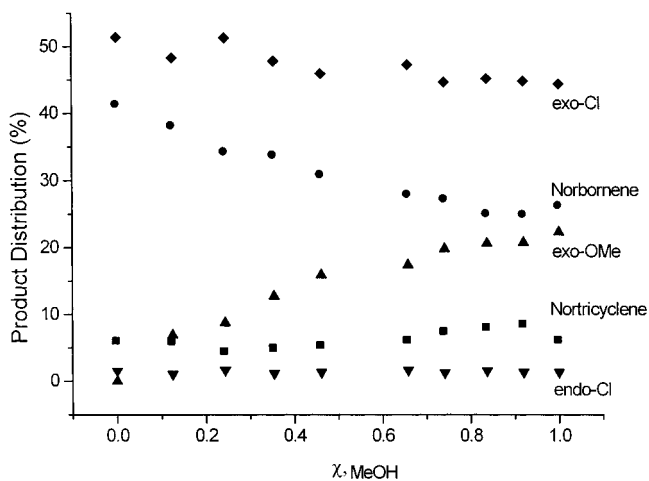
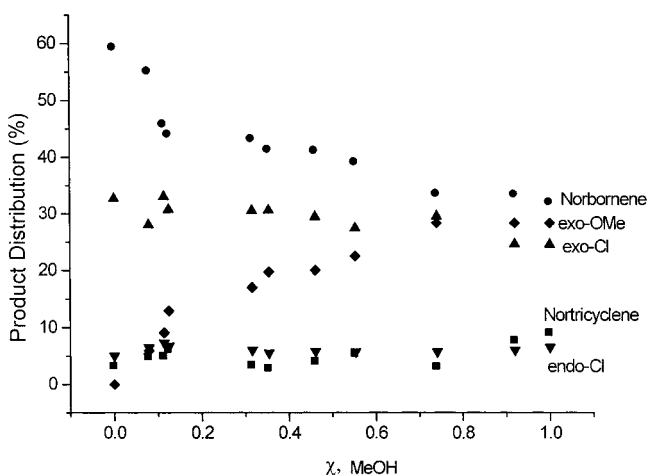


In Table 3, we collect the product distributions for the fragmentations of *exo-7* and *endo-7* in pure MeCN and pure MeOH. Two important observations can be made. (a) Even in pure MeOH, the formation of norbornyl chlorides **8** and **9** persists and is little diminished by the nucleophilic solvent. Similar persistence of “return” products was previously seen in the fragmentations of benzyloxylchlorocarbene²¹ and cyclo-

(19) A search of the literature did not locate reports of norbornene from solvolyses of **1** or **3**.

(20) With the primary *n*-BuOCCl, however, addition of 0.5 M TBACl in MeCN increased the yield of *n*-BuCl from 10.3 to 21.5%, whereas the combination of 0.5 M TBACl + 5.8 M pyridine increased the *n*-BuCl to 63.3%.^{12b} Here, S_N2 fragmentations are important.

(21) Moss, R. A.; Wilk, B. K.; Hadel, L. M. *Tetrahedron Lett.* **1987**, 28, 1969.

**Figure 1.** Product distribution (%) vs mole fraction of methanol (in MeCN) for the fragmentation of *exo-7*.**Figure 2.** Product distribution (%) vs mole fraction of methanol (in MeCN) for the fragmentation of *endo-7*.

propylmethoxychlorocarbene,²² and associated with the intermediacy of (R⁺OC⁻) ion pairs. (b) Ether **12** forms largely at the expense of norbornene, rather than chlorides **8** and **9**, as is clearly shown in Figure 1, where the yields of products **8–12** are correlated with the mole fraction of MeOH in solvent MeCN. The relative yields of chlorides **8** and **9** are effectively constant across the entire MeOH/MeCN regime, while the gradual increase of ether **12** is mirrored by a corresponding decrease in norbornene. Comparable behavior occurs in the fragmentations of *endo-7* in MeOH/MeCN (Figure 2), and of *exo-7* in MeOH/DCE (not shown).

These results suggest the intervention of at least two kinds of fragmentation intermediates: the first, a tight ion pair, can efficiently collapse to the chlorides, but cannot be readily trapped by methanol, while the second species can be diverted to ether **12** upon reaction with methanol. In fact, as discussed below, the likely participation of *syn* and *anti* forms¹¹ of *exo-* and *endo-7* further complicates the mechanistic analysis and enlarges the menagerie of possibly distinct ion pair intermediates.

Kinetics. LFP^{11,12,23} permitted the determination of rate constants for the fragmentations of *exo-7* and *endo-7* in MeCN and DCE solvents. Two monitoring methods were employed in the LFP studies: UV detection with pyridine ylide visualization,²⁴ and time-resolved infrared (TRIR) detection.^{12c,25}

(22) Moss, R. A.; Ho, G. J.; Wilk, B. K. *Tetrahedron Lett.* **1989**, 30, 2473.

(23) For a description of our LFP apparatus, see ref 12b.

Table 4. Rate Constants (k_{frag}) for the Fragmentations of *exo*- and *endo*-**7**^a

method	MeCN		DCE	
	<i>exo</i> - 7	<i>endo</i> - 7	<i>exo</i> - 7	<i>endo</i> - 7
LFP (UV)	<i>b</i>	4.8×10^5	7.2×10^4	8.7×10^4
LFP (TRIR) ^c	4.8×10^5	5.4×10^5	4.4×10^5	5.6×10^5

^a Rate constants in s^{-1} at 25 °C. ^b Not determined; see text. ^c CO formation was followed at 2132 cm^{-1} in DCE and 2140 cm^{-1} in MeCN.

In the UV-pyridine approach, carbenes **7** are generated via LFP of diazirines **6** at 351 nm. The fragmentations of the “invisible” carbenes are then followed in competition with their capture by added pyridine to form ylides **13** ($\lambda_{\text{max}} = 412 \text{ nm}$), where R = *exo*- or *endo*-2-norbornyl.

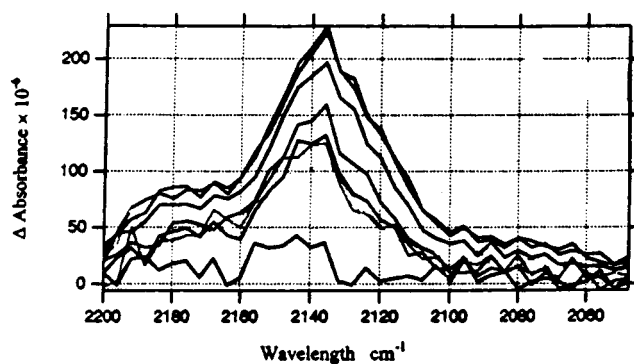
In DCE, a correlation of the apparent rate constants for ylide formation from *exo*-**7**, k_{obs} ($1.82\text{--}5.89 \times 10^5 \text{ s}^{-1}$), vs pyridine concentration (1.62–7.42 M) was linear (9 points, $r = 0.996$) with a slope of $6.07 \times 10^4 \text{ M}^{-1} \text{ s}^{-1}$, equivalent to the rate constant for ylide formation (k_y), and a *Y*-intercept of $7.23 \times 10^4 \text{ s}^{-1}$, equivalent to the rate constant for carbene fragmentation, k_{frag} . In the same manner, we examined the fragmentation of *endo*-**7**, obtaining a comparable linear correlation of k_{obs} vs [pyridine] (8 points, $r = 0.997$), which gave $k_y = 6.16 \times 10^4 \text{ M}^{-1} \text{ s}^{-1}$ and $k_{\text{frag}} = 8.68 \times 10^4 \text{ s}^{-1}$. The k_{frag} values appear in Table 4.

In MeCN, a correlation of k_{obs} for ylide formation ($0.538\text{--}0.970 \times 10^6 \text{ s}^{-1}$) from *endo*-**7** vs pyridine concentration (1.65–7.42 M) was linear (9 points, $r = 0.988$), and gave $k_y = 5.01 \times 10^4 \text{ M}^{-1} \text{ s}^{-1}$ with $k_{\text{frag}} = 4.76 \times 10^5 \text{ s}^{-1}$. Repetition of this determination led to a second value for k_{frag} ($4.79 \times 10^5 \text{ s}^{-1}$), yielding an average $k_{\text{frag}} = 4.78(\pm 0.02) \times 10^5 \text{ s}^{-1}$.

However, attempted correlation of the rate constants for ylide formation with pyridine concentrations for *exo*-**7** fragmentation in MeCN led to a *nonlinear* V-shaped plot. Related results have been observed for other *sec*-ROCCI in MeCN (but *not* in DCE).²⁶ We tentatively attribute this behavior to the effect on k_{frag} and k_y of changes in the solvent polarity as MeCN ($\epsilon = 35.6$) is diluted with pyridine ($\epsilon = 12.3$) over the full range of the k_{obs} vs [pyridine] LFP experiments. With DCE ($\epsilon = 10.7$), the effect of pyridine dilution on solvent polarity is mitigated, and linear correlations of k_{obs} with [pyridine] are consistently found.

The kinetics of fragmentation were also studied by LFP using TRIR methodology.^{12c,27} LFP of *exo*- or *endo*-**7** in MeCN or DCE was monitored from 2048 to 2200 cm^{-1} by TRIR spectroscopy using a 0.5 mm IR cell and $A_{355}(\mathbf{6}) = 0.44\text{--}0.50$. Figure 3 illustrates several IR scans collected over the time period 0 to 9 μs after the laser flash for the fragmentation of *exo*-**7** in DCE. CO formation is observed at 2132 cm^{-1} , and is equated with the fragmentation of ROCCI. The time dependence of the CO formation could be analyzed as a first-order phenomenon^{12c} to give $k_{\text{frag}} = 4.4 \times 10^5 \text{ s}^{-1}$; cf., Table 4.

The rate constants in Table 4 demonstrate reasonable agreement between k_{frag} values determined by either UV or TRIR monitoring methods. There are some differences between the rate constants for *exo*-**7** and *endo*-**7** as determined by TRIR or UV in DCE, with the TRIR values higher by ~ 6 -fold. Although

**Figure 3.** LFP-TRIR kinetics for the fragmentation of *exo*-**7** in DCE. Note the increasing formation of CO ($\nu_{\text{max}} 2132 \text{ cm}^{-1}$) in repetitive IR scans taken 0–9 μs after the laser flash.**Table 5.** Rate Constants (k_2 , $\text{M}^{-1} \text{ s}^{-1}$) for Fragmentations of *exo*- and *endo*-**7** in the Presence of Added Salts^a

salt ^b	solvent	k_2 (<i>exo</i> - 7)	k_2 (<i>endo</i> - 7)
TBACl	MeCN	3.0×10^6	1.3×10^5
TBACl	DCE	4.4×10^5	1.4×10^6
TBABF ₄	MeCN	6.2×10^5	4.3×10^5

^a Slopes of the correlations ($r > 0.98$, 6–8 points) of k_{obs} vs [salt] (see text) at 21.4 °C; monitored by UV (pyridine ylide methodology).

^b See Table 1, footnotes *b* and *d*.

we do not know the origin of this discrepancy, the important point is that the rate constants fall in a narrow range, 7.2×10^4 to $5.6 \times 10^5 \text{ s}^{-1}$; there is no kinetic advantage in fragmentation rate for *exo*-**7** vis-à-vis *endo*-**7** in either MeCN or DCE. Within experimental error, the *exo*-**7** and *endo*-**7** k_{frag} values are nearly identical.

Furthermore, these k_{frag} values are “normal” for *sec*-ROCCI fragmentations. Thus, cyclopentylloxycarbene, **14**, affords $k_{\text{frag}} = 8.7 \times 10^4 \text{ s}^{-1}$ (UV, DCE), $5.3 \times 10^5 \text{ s}^{-1}$ (TRIR, MeCN), and $6.1 \times 10^5 \text{ s}^{-1}$ (TRIR, DCE),²⁶ values comparable to those of *exo*- and *endo*-**7**.

The temperature dependence of k_{frag} for *exo*- and *endo*-**7** was studied from –40 to 30 °C in DCE using the pyridine ylide-UV monitoring method. Very poor correlations of $\ln k_{\text{frag}}$ vs $1/T$ were obtained. In our experience, this usually occurs when $E_a < 4 \text{ kcal/mol}$.

We also studied salt effects on k_{frag} . In these experiments, k_{obs} for the formation of ylide **13** was determined by LFP in MeCN or DCE solutions of *exo* or *endo* diazirines **6** containing a constant concentration of pyridine (5.77 M) and varying concentrations (0.042–0.504 M) of TBACl or TBABF₄. Linear correlations of k_{obs} and [salt] were observed, in which the slope expressed the sensitivity of k_{frag} to salt concentration. These values (k_2) are collected in Table 5. Note that at [salt] = 0, the *Y*-intercepts of these correlations should equal k_{obs} for ylide formation at [pyridine] = 5.77 M. These correspondences are observed.

Salt effects on k_{frag} are visible: increasing salt concentrations increase k_{frag} . However, because both TBACl and TBABF₄ exhibit this behavior, while added TBACl does not markedly increase the yields of chlorides **8** and **9** (Tables 1 and 2), we believe that the rate constants of Table 5 relate to salt effects on “S_N1” fragmentations of **7**; S_N2 reactions^{12b} of **7** and Cl[–] are not important.

Computational Studies. In analogy to our previous computational studies of alkoxyhalocarbene fragmentation,¹³ we computed ground states (GS) and fragmentation transition states (TS) for (cis) *exo*- and *endo*-norbornyloxycarbene (7). All structures were fully optimized by analytical gradient methods

(24) (a) Jackson, J. E.; Soundararajan, N.; Platz, M. S.; Liu, M. T. H. *J. Am. Chem. Soc.* **1988**, *110*, 5595. (b) Platz, M. S.; Modarelli, D. A.; Morgan, S.; White, W. R.; Mullins, M.; Celebi, S.; Toscano, J. P. *Prog. React. Kinet.* **1994**, *19*, 93.

(25) For methodological references, see ref 12c, note 10.

(26) Moss, R. A.; Johnson, L. A. Unpublished studies.

(27) Wang, Y.; Yuzawa, T.; Hamaguchi, H.; Toscano, J. P. *J. Am. Chem. Soc.* **1999**, *121*, 2875.

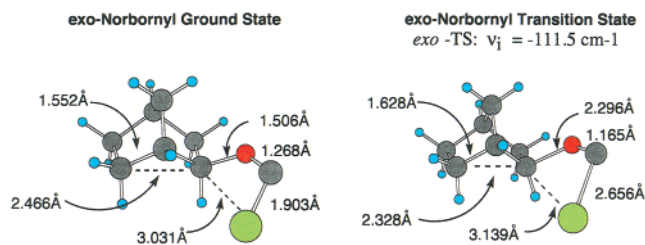


Figure 4. B3LYP/6-31G* ground and fragmentation transition states for *exo-7*.

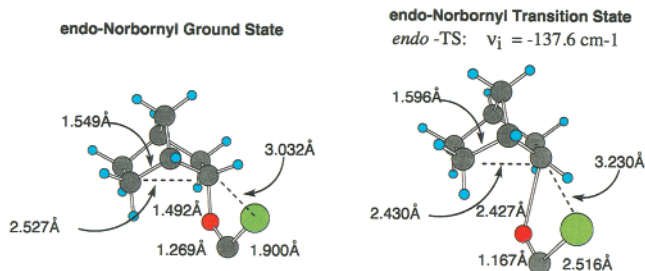


Figure 5. B3LYP/6-31G* ground and fragmentation transition states for *endo-7*.

at the B3LYP/6-31G* level using the Gaussian94 and Gaussian98 suites of programs.²⁸ Computed (unscaled) gas-phase energies were corrected for thermal effects at 298.15 K and for zero-point energy differences. Normal coordinate analyses confirmed the nature of the GS and TS structures. Calculations of energies in simulated MeCN solvent employed the SCI-PCM computational model with single point calculation based on the fully optimized gas-phase geometry.

The computed GS and TS structures for *exo-7* and *endo-7* (in MeCN) appear in Figures 4 and 5, respectively. In each TS, the C–Cl and (alkyl) C–O bonds are in the process of breaking: C–Cl distances increase from 1.90 to 2.66 Å (*exo-7*) and from 1.90 to 2.52 Å (*endo-7*), while parallel increases occur in the C–O distances, 1.51 to 2.30 Å (*exo-7*) and 1.49 to 2.43 Å (*endo-7*). Simultaneously, the carbene C–O bonds each contract from 1.27 to 1.16–1.17 Å, enroute to the 1.128 Å bond length of CO.

Note the proximity of the nascent Cl[−] anion and C2^{δ+} in each TS, 3.14 Å for *exo-7* and 3.23 Å for *endo-7*, which points toward the subsequent formation of ion pairs (see below). We also observe small increases (0.04–0.08 Å) in the C1–C6 bond lengths, and corresponding decreases (0.10–0.14 Å) in the C2–C6 separations, as the *endo-7* or *exo-7* GS moves to its fragmentation TS. Alterations in the C1–C7 bonds²⁹ between GS and TS are very small (0.01–0.02 Å).

The bond length alterations are all in accord with concerted C–O and C–Cl heterolyses whereby *exo-7* and *endo-7* fragment to ion pairs. Note, however, that the C1–C6 and C2–C6 distances in our TS structures, 1.59–1.63 and 2.33–2.43 Å, respectively, are still significantly different from each other and from the final value of ~1.83 Å that they will both approach in the nonclassical 2-norbornyl cation.^{4c}

Activation energies were obtained for the fragmentations of *exo-7* and *endo-7* in MeCN as differences between the computed

TS and GS energies, affording $E_a = 0.74$ (*exo-7*) and 2.46 kcal/mol (*endo-7*).²⁹ Although there appears to be a residual exo advantage here, the computed ΔS^\ddagger values (7.0 eu for *exo-7* and 1.0 eu. for *endo-7*) lead to $\Delta G^\ddagger = 2.60$ and 2.87 kcal/mol, respectively, for the fragmentations at 298 K; a prediction of comparable k_{frag} values for the isomeric carbenes is, in fact, observed (Table 4).

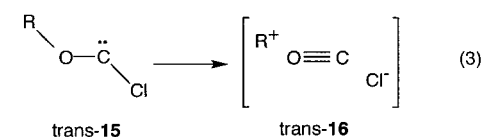
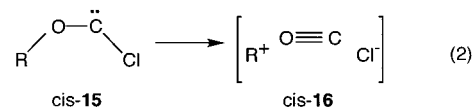
The small computed E_a values are in agreement with the observed rapid fragmentations of the carbenes and with comparatively “early” transition states (Figures 4 and 5). The computed activation energies for the fragmentations of *exo-* and *endo-7* in MeCN are lower than that calculated (in MeOH) for (cis) Me₂CHOCCI (8.0 kcal/mol), but similar to the calculated E_a for the fragmentation of PhCH₂OCCI (1.4 kcal/mol).¹³

Discussion

This Discussion is restricted to those components of the Results which appear to require further exposition. The key questions posed at the beginning of this report can now be answered. First, when the leaving group is made so reactive that, as in these carbene fragmentations, E_a for the C–X heterolysis approaches zero, the kinetic disparity between the *exo-* and *endo-2-norbornyl* substrates does indeed disappear. The k_{frag} values for *exo-* and *endo-7* are virtually identical (Table 4), while the computed E_a values are <3 kcal/mol. Although we were unable to obtain good enough experimental data to determine the E_a values, indications are that they are less than ~4 kcal/mol. The extraordinary reactivity of the fragmenting OCCl leaving group minimizes electron demand on the C1–C6 σ bond, so that the isomeric carbenes **7** fragment to the norbornyl ion pairs at similar rates, which are not elevated in comparison to the fragmentation of a “normal” *sec*-ROCCI, e.g., **14**.

Second, in this low activation energy regime, differences between the ions or ion pairs initially formed from *exo-* or *endo-7* are reflected in their respective product distributions; cf., Tables 1–3 and Figures 1 and 2. To assess the product distributions, we must briefly revisit the mechanism of carbene fragmentation.

There is substantial evidence from anion return, stereochemistry, and cyclopropylcarbiny/cyclobutyl rearrangements that the fragmentations of most ROCCI proceed via ion pairs.^{11,21,22,30} However, the initially formed ion pair could be “cis” or “trans”, depending on the geometry of the precursor carbene,¹¹ cf., eqs 2 and 3. Rotation about the central O–C bond of ROCCI is opposed by ~15–18 kcal/mol due to partial double bond



character.^{13,31} It is possible that *cis-16*, in which CO does not insulate R⁺ from Cl[−], might be largely responsible for the RCl products formed by ion pair return in MeOH (Table 3), whereas

(28) Gaussian, Inc.: Pittsburgh, PA. DFT calculations employed Becke’s three-parameter hybrid method with the LYP correlation functional: Becke, A. D. *J. Chem. Phys.* **1993**, *98*, 5648.

(29) Schleyer et al. reported computed (B3LYP/6-311+G**/B3LYP/6-31G*) activation energies for the ionization of protonated *exo-* and *endo-2-norborneols* (**1** and **3**, X = OH₂⁺): $E_a(\text{exo}) = 2.8$ kcal/mol and $E_a(\text{endo}) = 5.3$ kcal/mol. Cf.: Schreiner, P. R.; Schleyer, P. v. R.; Schaefer, H. F., III *J. Org. Chem.* **1997**, *62*, 4216.

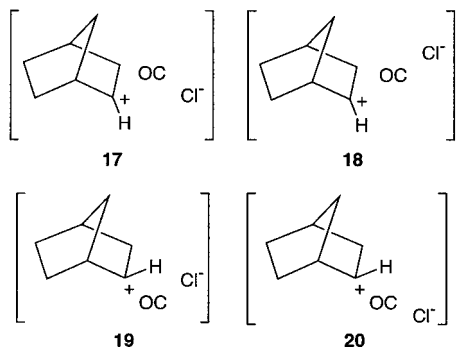
(30) Moss, R. A.; Balcerzak, P. *J. Am. Chem. Soc.* **1992**, *114*, 9386.

(31) For examples of ROCCI isomers, see: Kesselmayr, M. A.; Sheridan, R. S. *J. Am. Chem. Soc.* **1986**, *108*, 99 and 844.

trans-**16**, in which CO separates R⁺ from Cl⁻, might be more readily captured by MeOH, mainly yielding solvolysis product **12**.

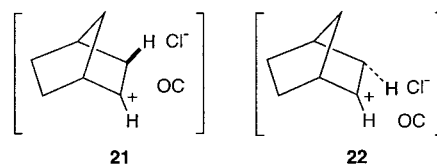
Now consider the products formed by the fragmentations. These reactions are rapid ($k_{\text{frag}} \sim 7 \times 10^4$ to $6 \times 10^5 \text{ s}^{-1}$, Table 4), have very low activation energies, and are modestly accelerated by added TBACl or TBABF₄ (Table 5). The overall behavior is consistent with the ion pair formulation of eqs 2 and 3,¹¹ where unimolecular fragmentation is faster than bimolecular trapping of the carbenes by MeOH or Cl⁻. Only fragmentation products **8–12** are observed in DCE, MeCN, or MeOH (Tables 1–3); trapping products such as ROCHCl₂ or formates are absent.

Given the *exo* and *endo* configurations of **7**, the *cis* and *trans* isomerism possible for its O–C–Cl “leaving group”, and the conformational possibilities due to rotation about the R–OCCl bond, there may well be a family of nearly isoenergetic but geometrically variant ion pairs initially formed upon fragmentation of *exo*- or *endo*-**7**. For simplicity, we draw four representative ion pairs, **17–20**, corresponding to fragmentations of *exocis* (**17**), *exo-trans* (**18**), *endocis* (**19**), and *endo-trans* (**20**) forms of carbene **7**.

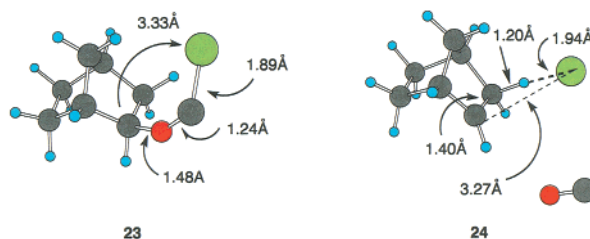


It is possible that ion pairs **17–20** become nonclassical on the vibrational time scale but, for “*cis*” ion pairs **17** and **19**, cation/anion collapse might be competitive with evolution to the fully bridged 2-norbornyl cation. Ion pair **17** will efficiently decay to *exo*-chloride **8**, and will likely be unaffected by the addition of MeOH. It is responsible for the approximately constant yield of **8** formed in various mixtures of MeOH in MeCN (Table 3, Figure 1). Ion pair **18**, however, would be less likely to yield **8**; escape to a solvated 2-norbornyl cation (with eventual formation of ether **12**) is possible here. Ion pair **19** should largely collapse to chlorides **8** and **9**, but its initial geometry confers some bias toward *endo*-chloride **9**. This outcome is opposed by the nonclassical evolution of the cation, so that *exo*-chloride **8** remains the dominant chloride formed. The chlorides derived from **19**, however, will be relatively unaffected by MeOH addition (Table 3, Figure 2). We should expect a smaller *exo*-Cl/*endo*-Cl (**8/9**) product ratio from chloride return of **19** or **20** than from the analogous process of **17** or **18**. Indeed, the observed **8/9** ratios are 4.6 vs 41.4 from *endo*-**7** vs *exo*-**7** in MeCN (4.6 vs 25.2 in DCE).

A major feature of these fragmentations is the very large quantity of norbornene (**10**) formed from *exo*-**7** and (even more so) *endo*-**7** (Tables 1 and 2), in marked contrast to solvolytic reactions of 2-norbornyl sulfonates.¹⁹ Much of the norbornene could arise via proton transfers from C3 to Cl⁻ within the ion pairs. Ion pairs such as **21** or **22** would appear to favor proton transfers (i.e., elimination to **10**), and could arise either by reorganizations within **17–20** or directly by fragmentations of alternative conformations of *cis* or *trans* *exo*- or *endo*-**7**. To probe



whether other conformations of the oxychlorocarbenes could be involved in norbornene formation, we located a higher energy conformer of *exo*-2-norbornyloxylchlorocarbene (**23**) which placed the chloride atom in close proximity to the appropriate *exo*-hydrogen atom (cf., **21**). Several attempts were made to locate fragmentation transition states from **23**. Depending on the initial geometry, trial structures decayed either to the transition structure shown in Figure 4 or to assemblage **24**. The latter was generated via a barrierless process, i.e., energy decreased monotonically to a point lower in overall energy than the initial carbene itself. The incipient formation of norbornene, HCl, and carbon monoxide are clearly apparent in **24**. These results are consistent with our other suggestions concerning the origins of norbornene.



We also recall that the dilution of solvent MeCN by MeOH generates capture product **12** largely at the expense of norbornene (Figures 1 and 2, Table 3). Ion pairs **21** or **22** would appear to be appropriate candidates to partition between proton transfer affording norbornene or MeOH capture yielding **12**.

We should also comment on the likelihood of a “S_Ni” mechanism for the conversions of *exo*-**7** to **8** and *endo*-**7** to **9**. In 1971, Tabushi³² described a phase transfer catalytic version of the Hine–Skell “deoxidation” reaction,³³ in which CCl₂ (generated from chloroform, 50% aqueous NaOH, and a catalytic quantity of benzyltriethylammonium chloride) converted alcohols to alkoxychlorocarbenes and thence, by fragmentation, to alkyl chlorides. Tabushi applied these conditions to the norborneols, generating *exo*- and *endo*-**7**. From *exo*-norborneol, 90% of *exo*-chloride was obtained, whereas *endo*-norborneol afforded 47% of *exo*- and 44% of *endo*-chloride!³² Norbornene was *not* reported as a product. These results, taken together with those for analogous reactions of other alcohols, led to a suggestion that “the S_Ni mechanism may be operative,” albeit with “considerable leakage to a carbonim ion...”³²

Later, Jones et al. proposed a related mechanism to account for the formation of a 70–80% *exo* mixture of epimeric chlorides in the CCl₂-mediated ROCCl fragmentations of either epimer of a pair of tricyclic alcohols related to the 2-norborneols. In their view, the S_Ni reactions “involve a carbocation which is committed to chloride formation through intramolecular capture with retention.”³⁴

We repeated the CCl₂ “deoxidation” of *endo*-2-norborneol.³² In our case, the product mixture comprised 39.5% of **8**, 4.7%

(32) Tabushi, I.; Yoshida, Z.-i.; Takahashi, N. *J. Am. Chem. Soc.* **1971**, *93*, 1820.

(33) Hine, J.; Pollitzer, E. L.; Wagner, H. *J. Am. Chem. Soc.* **1953**, *75*, 5607. Skell, P. S.; Starer, I. *J. Am. Chem. Soc.* **1959**, *81*, 4117.

(34) Likhovotvorik, I. R.; Jones, M., Jr.; Yurchenko, A. G.; Krasutsky, P. A. *Tetrahedron Lett.* **1989**, *30*, 5089.

of **9**, and 55.8% of **10**. Controls demonstrated the stability of the reaction products to the experimental conditions. The observed product distribution resembles that obtained from the fragmentation of diazirine-derived *endo-7* in DCE with added TBACl (Table 2). The reported³² large yield of *endo*-chloride and the absence of norbornene were not reproduced. The ion pair mechanism for the fragmentations of carbenes **7**, as described above, remains our preferred rationale.

In conclusion, the fragmentations of *exo*- and *endo*-2-norbornyloxylchlorocarbenes occur at similar rates and transit low energy barriers which lead to little *exo/endo* kinetic differentiation. Ion pairs are formed which are geometrically akin to the configuration and conformation of their precursor carbenes; product distributions from *exo*- and *endo-7* therefore differ. In both cases, large quantities of norbornene form via proton transfer from C3 to the chloride anion within the ion pairs. The ion pairs that lead to norbornene can be competitively intercepted by added methanol.

Experimental Section

Solvents. Acetonitrile (Fischer, Certified A. C. S.) and pyridine (Fisher, Certified A.C.S.) were dried by reflux over CaH₂, followed by distillation and storage over 5A molecular sieves. Dichloroethane (DCE) (Aldrich, Certified A.C.S.) was used without further treatment. Pentane (Fisher, HPLC grade) was stored over 5A molecular sieves.

exo-2-Norbornylisouronium Trifluoromethanesulfonate (exo-5). This material was prepared using the procedure described in ref 14.

endo-2-Norbornylisouronium trifluoromethanesulfonate (endo-5). In a 50 mL one-neck round-bottom flask, equipped with a stirring bar and a reflux condenser protected with a calcium chloride tube, were placed 1.00 g (23.8 mmol) of cyanamide, 5.34 g (47.6 mmol) of *endo*-norborneol, and 12 mL of anhydrous THF. To this solution was added 3.57 g (23.8 mmol) of trifluoromethanesulfonic acid. The mixture was magnetically stirred at 55 °C (oil bath) for 30 h. After the reaction mixture had been cooled to room temperature, it was diluted with 200 mL of pentane and refrigerated. A brown solid was harvested and washed with 6 × 15 mL of ether to afford white crystals that were dried under vacuum (25 °C, <1 Torr). We obtained 2.53 g of *endo-5*, mp 109–111 °C. ¹H NMR (δ, DMSO-*d*₆): 0.99–2.20, 2.48–2.67 (m's, 10 H, norbornyl); 4.87–5.02 (m, 1 H, CHO); 8.43 (br s, 4 H, 2NH₂). Anal. Calcd for C₉H₁₅F₃N₂O₄S: C, 35.5; H, 4.93; N, 9.21. Found: C, 35.2; H, 4.66; N, 9.42.

3-Chloro-3-(exo-2-norbornyloxy)diazirine (exo-6). The general procedure of Graham¹⁵ was followed. To 3.5 g of LiCl in DMSO was added 1.0 g (3.3 mmol) of isouronium salt (*exo-5*) and 50 mL of pentane. The mixture was cooled to 20 °C and stirred magnetically. Then, 200 mL of 12% commercial aqueous sodium hypochlorite solution, saturated with NaCl, was slowly added. After the addition was complete, stirring was continued for 15 min at 15 °C. The reaction mixture was transferred to a separatory funnel containing 150 mL of ice water, the aqueous phase was removed, and the pentane phase was washed twice with ~75 mL of ice water and then dried for 2 h over CaCl₂ at 0 °C. The pentane/diazirine solution was purified by chromatography over Aldrich 200–400 mesh, 60 Å, silica gel, eluted with pentane. The volume of pentane was reduced by rotary evaporation, and replaced by acetonitrile (or DCE). The remaining pentane was then removed by rotary evaporation at 0 °C. About 30 mL of an acetonitrile (or DCE) solution of diazirine *exo-6* resulted. ¹H NMR (δ, CD₃CN): 0.7–1.7, 2.15–2.25 (m's 10 H, norbornyl); 3.90–4.00 (m, 1 H, CHO). UV (pentane), λ_{max} 359 nm. The yield of *exo-6* was ca. 50%.

3-Chloro-3-(endo-2-norbornyloxy)diazirine (endo-6). This material was prepared from isouronium salt *endo-5* exactly as described for the isomeric diazirine, *exo-6*. ¹H NMR (δ, CD₃CN): 0.70–1.50, 1.50–1.70 (m's, 10 H, norbornyl); 3.96–4.12 (m, 1 H, CHO). UV (pentane), λ_{max} 352 nm. The yield of *endo-6* was ca. 50%.

endo-2-Norbornyl Chloride (9).³⁵ In a 50 mL round-bottom flask, fitted with a reflux condenser, was placed 1.0 g (8.9 mmol) of *exo*-

norborneol, 3.54 g (13.6 mmol) of triphenylphosphine, and 20 mL of CCl₄. The mixture was refluxed for about 2 h and then cooled to room temperature. The CCl₄ was distilled off and the residue was extracted with 20 mL of acetonitrile. The volume of acetonitrile was reduced to about 5 mL by rotary evaporation. The resulting MeCN solution of 2-norbornyl chlorides was analyzed by GC and GC-MS; the ratio of *exo*- and *endo*-2-norbornyl chlorides (**8/9**) was 1.5/1. The *exo* chloride was coeluted with a commercial sample (Aldrich).

Nortricyclene.³⁶ Norcamphor tosylhydrazone was prepared by combining *p*-toluenesulfonylhydrazine (2.7 g, 14.5 mmol) and 1.6 g (14.5 mmol) of norcamphor in 30 mL of 1% sulfuric acid in ethanol. The solution was heated (55 °C, 5 min), poured into ice water, and allowed to crystallize, affording the tosylhydrazone in near quantitative yield; mp 200–202 °C, lit.³⁶ mp 201.5–202.5 °C.

A three-neck flask was equipped with a magnetic stirring bar, dropping funnel, nitrogen inlet, and a 30 cm Vigreux column. The latter was connected to a series of 2 traps which were cooled with dry ice–acetone. Nitrogen gas was led through the inlet and served to sweep the volatile reaction products into the traps. A suspension of 1.93 g (37 mmol) of sodium methoxide was suspended in 25 mL of diglyme and heated in the flask to 160 °C. A solution of 3.0 g (11 mmol) of norcamphor tosylhydrazone in 50 mL of diglyme was added dropwise over 1.5 h to the hot base. Then, the contents of the two traps were diluted with ~15 mL of water and extracted with 3 × 15 mL of pentane. The combined pentane extract was dried over CaCl₂, filtered, and freed of pentane by careful distillation, yielding 0.41 g (40%) of nortricyclene. ¹H NMR³⁷ (δ, CDCl₃): 0.97 (s, 3 H, H1, H2, H6); 1.19 (s, 6 H, 2H3, 2H5, 2H7); 1.91 (s, 1 H, H4).

exo-2-Norbornyl Methyl Ether (12).³⁸ To 0.94 g (10 mmol) of norbornene and 0.48 g (15 mmol) of methanol in 10 mL of dry CH₂-Cl₂ was added 1.23 mL (10 mmol) of BF₃·etherate. The mixture was stirred for 15 min at 25 °C and then quenched by addition of 20 mL of aqueous NaHCO₃. The organic phase was retained; the aqueous layer was extracted with 3 × 5 mL of CH₂Cl₂; the organic phase and the extracts were combined. Drying (CaCl₂), filtration, and rotary evaporation were followed by short-path distillation (60–62 °C, 15 Torr) to give 1.25 g (64%) of **12**. ¹H NMR (δ, CDCl₃): 0.92–1.13, 1.29–1.60 (m's, 8 H, norbornyl); 2.22 and 2.33 (m's, 1 H each, bridgeheads); 3.26, (s, 3 H, CH₃); 3.20–3.80 (m, 1 H, CHO).

Photolysis of Diazirines. LFP experiments employed the system described in detail in ref 12b. LFP-TRIR experiments were performed at Johns Hopkins University.²⁵ For all product studies, solutions of *exo*- or *endo-6* in MeCN or DCE (*A*₃₅₆ = 1.0) were photolyzed at 25 °C for 1 h with a focused Oriel lamp, λ > 320 nm (uranium glass filter).³⁹ The products were analyzed by capillary GC (or GC-MS) using a 30 m × 0.25 mm (o.d.) × 0.25 μm (i.d.) CP-Sil 5CB (100% dimethyl polysiloxane) column at 40 °C (3 min), programmed to 150 °C at 10 deg/min. Products are described above; see Tables 1–3. Product identities were confirmed by GC and GC-MS comparisons to authentic samples.

Phase Transfer Catalytic Generation of endo-7.³² A mixture of *endo*-norborneol (0.56 g), 10 mL of 50% aqueous sodium hydroxide solution, and 0.02 g of benzyltriethylammonium chloride was stirred vigorously at 40 °C to emulsify it, and then 8 mL of CHCl₃ was added dropwise into the emulsion over 1 h. The mixture was stirred for a further 2 h and then extracted with 20 mL of ether and washed with water. The ether solution was analyzed by GC, which indicated the presence of norbornene (55.8%), *exo*-norbornyl chloride (39.5%), and *endo*-norbornyl chloride (4.7%). The products were identified by GC comparisons to authentic samples. In a control experiment, a mixture of *exo*- and *endo*-chlorides (**8/9** = 1.5) was vigorously stirred at 40 °C with 50% aqueous NaOH solution and 20 mg of benzyltriethylammo-

(36) Freeman, P. K.; George, D. E.; Rao, V. N. M. *J. Org. Chem.* **1964**, *29*, 1682.

(37) Kropp, P. J.; Adkins, R. L. *J. Am. Chem. Soc.* **1991**, *113*, 2709.

(38) Shellhamer, D. F.; Callahan, R. P.; Heasley, V. L.; Druelinger, M. L.; Chapman, R. D. *Synthesis* **1997**, 1056.

(39) Photolyses that included added salts or MeOH were carried out in the same manner. In a control experiment, *exo*-chloride **8** was shown to be stable in 1:1 MeOH/MeCN under the photolysis conditions.

(35) Weiss, R. G.; Snyder, E. I. *Chem. Commun.* **1968**, 1358.

nium chloride for 3 h, and then extracted with ether. The ether extract was washed with water and analyzed by GC, which showed that the **8/9** ratio remained 1.5/1.

Acknowledgment. This paper is dedicated to Professor Ronald Breslow on the occasion of his 70th birthday. We are grateful to Ms. Lauren A. Johnson and Mr. Brett M. Showalter

for technical assistance. We thank the National Science Foundation for financial support. J.P.T. acknowledges a NSF Faculty Early Career Development Award. Access to the computational resources of the Center for Computational Neuroscience at Rutgers University (Newark) is much appreciated.

JA010598Q